American Journal of Pathology, Vol. 164, No. 6, June 2004

Kinetics of Gene Expression in Murine Cutaneous Graft-*versus*-Host Disease

Philip B. Sugerman,* Sara B. Faber,*
Lucy M. Willis,† Aleksandra Petrovic,†
George F. Murphy,‡ Jacques Pappo,*
David Silberstein,* and
Marcel R. M. van den Brink†

From AstraZeneca Research and Development Boston, Waltham, Massachusetts; the Department of Medicine,† Memorial Sloan-Kettering Cancer Center, New York, New York; and the Department of Pathology,‡ Jefferson Medical College, Thomas Jefferson University, Philadelphia, Pennsylvania*

The kinetics of gene expression associated with the development of cutaneous graft-*versus*-host disease (GVHD) were examined in a mouse model of MHC-matched allogeneic hematopoietic stem cell transplantation. Ear skin was obtained from recipient mice with or without GVHD between 7 and 40 days after transplantation for histopathological analysis and gene expression profiling. Gene expression patterns were consistent with early infiltration and activation of $CD8^+$ T and mast cells, followed by $CD4^+$ T, natural killer, and myeloid cells. The sequential infiltration and activation of effector cells correlated with the histopathological development of cutaneous GVHD and was accompanied by up-regulated expression of many chemokines and their receptors (CXCL-1, -2, -9, and -10; CCL-2, -5, -6, -7, -8, -9, -11, and -19; CCR-1 and CCR-5), adhesion molecules (ICAM-1, CD18, Ly69, PSGL-1, VCAM-1), molecules involved in antigen processing and presentation (TAP1 and TAP2, MHC class I and II, CD80), regulators of apoptosis (granzyme B, caspase 7, Bak1, Bax, and *Bcl*II), interferon-inducible genes (STAT1, IRF-1, IIGP, GTPI, IGTP, Ifi202A), stimulators of fibroblast proliferation and matrix synthesis (interleukin-1β, transforming growth factor-β1), and markers of keratinocyte proliferation (keratins 5 and 6), and differentiation (small proline-rich proteins 2E and 1B). Many acute-phase proteins were up-regulated early in murine cutaneous GVHD including serum amyloid A2 (SAA2), SAA3, serpins a3g and a3n, secretory leukocyte protease inhibitor, and metallothioneins 1 and 2. The kinetics of gene expression were consistent with the evolution of cutaneous pathology as well as with current models of disease progression during cutaneous GVHD. *(Am J Pathol 2004, 164:2189–2202)*

Graft-*versus*-host disease (GVHD) is a common serious complication after allogeneic hematopoietic stem cell transplantation (HSCT) and is a major cause of HSCT-related mortality.[1] Acute GVHD occurs in humans within the first 100 days of transplantation and comprises dermatitis, enteritis, and hepatitis with immunosuppression and cachexia. Chronic GVHD develops after day 100 and comprises an autoimmune-like syndrome comparable to ulcerative colitis, primary biliary cirrhosis, Sjögren's syndrome, rheumatoid arthritis, and lupus-like disease with glomerulonephritis. The skin is a primary target in chronic GVHD and exhibits either a lichenoid eruption or scleroderma. Experimental murine GVHD elicited by minor histocompatibility antigenic differences in H2-identical transplants has proven to be an informative model for evaluating the pathogenesis of human disease.[2,3] The pathophysiology of GVHD consists of a cascade of humoral and cellular interactions between donor and host cells and involves spatial and temporal expression patterns of a variety of genes involved in inflammation, antigen presentation, effector cell recruitment and activation, apoptosis, and tissue repair. Most analyses of this complex process have focused on a limited number of cell types or molecules. We hypothesized that the kinetic analysis of global gene expression profiles using microarray gene expression technology could provide valuable information about the mechanisms involved in the development of cutaneous GVHD. Therefore, we examined the clinical and histopathological development of cutaneous GVHD in a clinically relevant mouse model of MHC-matched allogeneic HSCT and analyzed whole skin samples using microarray gene expression technology.

Supported by the National Health and Medical Research Council (Australia) Industry (research fellowship grant 143125 to P.B.S.), the National Institutes of Health (grants HL69929 and HL72412 to M.R.M.v.d.B. and CA40358 to G.F.M.), and the Leukemia and Lymphoma Society (translational research grant to M.R.M.v.d.B.).

M.R.M.v.d.B. is the recipient of a Damon Runyan Scholar Award of the Cancer Research Fund and a research award from the V scholar program of the V Foundation.

Accepted for publication February 19, 2004.

Supplemental data for this article appears at http://www.amjpathol.org.

Address reprint requests to Marcel R. M. van den Brink, M.D., Ph.D., Memorial Sloan-Kettering Cancer Center, Mailbox 111, 1275 York Ave., New York, NY 10021. E-mail address: m-van-den-brink@ski.mskcc.org.

Materials and Methods

Mice and HSCT

Protocols were approved by the Memorial Sloan Kettering Cancer Center Animal Care and Use Committee. Female donor B10.BR/SgSnJ and recipient CBA/J mice (both $H2^k$ haplotype) (Jackson Laboratory, Bar Harbor, ME) were between 8 to 12 weeks of age.[2,3] Donor bone marrow (BM) was removed aseptically from femurs and tibias and depleted of T cells with anti-Thy-1.2 antibody (30H.12) and low-TOX-M rabbit complement (Cedar Lane Laboratories, Hornby, Ontario, Canada). Donor splenic T cells were obtained by purification over nylon wool. T cell-depleted BM cells (5×10^6) with (GVHD) or without (control) 1×10^6 splenic T cells were transplanted by tail vein infusion into lethally irradiated (1300 cGy in two doses; ^{137}Cs source) recipient mice. Mice were sacrificed on days 7, 14, 21, or 40 after HSCT. Survival was monitored daily and ear-punched mice were individually scored weekly for five clinical parameters (weight loss, hunched posture, activity level, fur ruffling, and skin lesions) on a scale from 0 to 2. A clinical GVHD score was generated by the summation of the five criteria scores as described previously and mice scoring 5 or greater were sacrificed.[4] Unpunched ears were harvested and sectioned longitudinally for gene expression profiling and histopathological assessment. Four of 20 GVHD mice (days 7, 8, 19, and 20 after HSCT) and 1 of 16 control mice (day 40 after HSCT) died and were excluded from further investigation. Hence, data were obtained from four GVHD and four control mice on days 7, 14, and 21 after HSCT and four GVHD and three control mice on day 40 after HSCT.

Gene Expression

Total RNA was isolated from the ears (RNeasy; Qiagen, Valencia, CA). Double-stranded cDNA was synthesized from 10 μg of total RNA (Superscript Choice; Invitrogen, Carlsbad, CA) and isolated by phase-lock gel centrifugation (Eppendorf, Hamburg, Germany). Biotin-labeled cRNA was synthesized (Enzo BioArray; Affymetrix, Santa Clara, CA), cleaned (RNeasy, Qiagen), and fragmented. Hybridization cocktail was prepared (GeneChip Eukaryotic Hybridization Control, Affymetrix) and incubated with the U74Av2 probe array (Affymetrix) for 16 hours at 45°C and 60 rpm. Arrays were stained and scanned and the overall fluorescence intensity adjusted to a target intensity value (TIV) of 150. Fluorescence images were analyzed (Affymetrix) to generate an expression signal for each probe set.

Quality Control and Analysis

RNA quality was assessed by 260 nm:280 nm absorption (Spectramax Plus 384; Molecular Devices, Sunnyvale, CA) at five points, and by electrophoresis (RNA 6000 LabChip; Agilent Technologies, Palo Alto, CA) at three points throughout the assay. Hybridization quality was assessed visually and electronically using standard Affymetrix measures. Scaling factors for the TIV adjustment were comparable between all hybridizations. The 3′:5′ signal ratios for housekeeping genes (β-actin, GAPDH) were calculated for all hybridizations. Hybridizations with ratios greater than 5, indicating excessive RNA degradation, were excluded from further analysis. Within a complex RNA background, the reliable lower limit of transcript detection is 1 pmol/L.[5] In the present study, biotin-labeled *Escherichia coli* BioB cRNA (1.5 pmol/L) was spiked into every sample immediately before hybridization. Genes with a mean expression value below the limit of detection (defined as 2/3 mean BioB signal) in both GVHD and control groups were excluded from further analysis. Differences in gene expression between GVHD and control groups were analyzed by Wilcoxon rank sum test, with only maximum rank sum differences considered significant.

Enzyme-Linked Immunosorbent Assay (ELISA)

In parallel experiments, GVHD and control ears were harvested and homogenized in 4× phosphate-buffered saline-Tween buffer using a PowerGen 125 laboratory homogenizer (Fisher Scientific, Pittsburgh, PA). The homogenate was centrifuged at 14,000 rpm for 10 minutes and the supernatant stored at −80°C. The concentration of RANTES protein in the homogenate was determined by ELISA (R&D Systems, Minneapolis, MN) according to the manufacturer's instructions.

Histopathological Evaluation

Ear skin was semiquantitatively graded according to the following criteria based on our experience with sequential pathological alterations that occur in this murine model:[3,6] grade 0: no infiltrate or injury (normal skin); grade 1: no infiltrate, mast cell degranulation, or superficial dermal lymphoid infiltrate, no significant epidermal changes or exocytosis; grade 2: lymphoid exocytosis into epidermis, focal to diffuse epidermal hyperplasia, apoptosis <1/10 basal cells; grade 3: lymphoid exocytosis, diffuse epidermal hyperplasia, apoptosis 1 to 2/10 basal cells; grade 4: lymphoid exocytosis, diffuse epidermal hyperplasia, apoptosis >2/10 basal cells.

Results

Clinical and Histological GVHD

We used a well-described MHC-matched murine allogeneic HSCT model with a disparity in minor histocompatibility antigens (mHAgs): B10.BR → CBA/J.[2] In this model, the addition of donor T cells to the T cell-depleted BM graft (TCD-BM) causes GVHD in recipient mice, whereas mice that receive only TCD-BM do not develop GVHD. We chose this model because of its clinical relevance and resemblance to GVHD in patients receiving an allogeneic HSCT from a MHC-matched unrelated donor. We added a T-cell dose to the TCD-BM graft that would

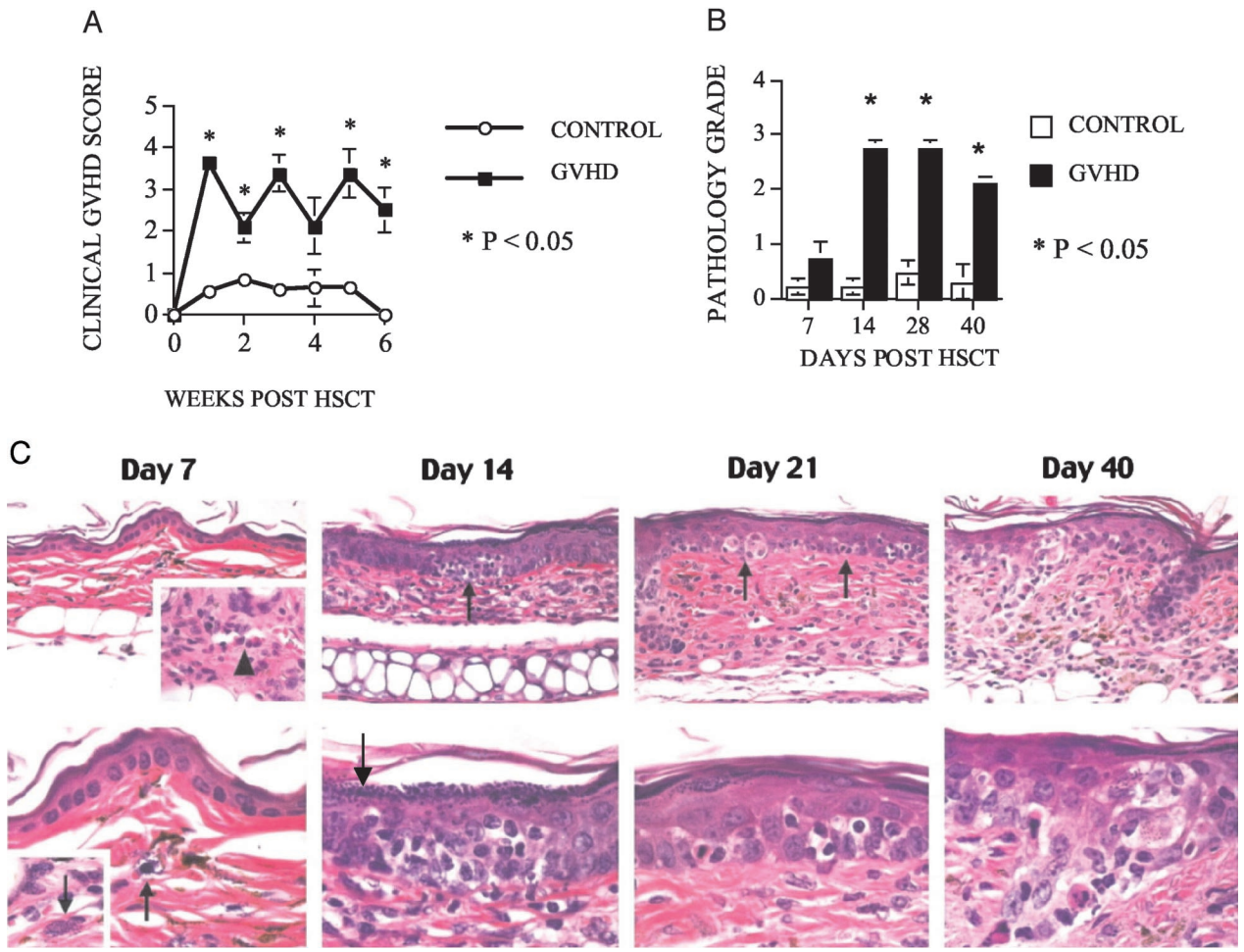

Figure 1. Lethally irradiated recipients of allogeneic TCD-BM with T cells develop systemic and cutaneous GVHD by clinical and histopathological criteria. Lethally irradiated (1300 cGy) CBA/J recipients received TCD-BM cells (5×10^6) with (GVHD) or without (control) 1×10^6 splenic T cells. **A:** Clinical GVHD was determined weekly using a semiquantitative scoring system as described in Materials and Methods. **B:** Four mice per group were sacrificed on days 7, 14, and 21 after HSCT and four GVHD and three control mice on day 40 after HSCT. Ears were harvested for semiquantitative histopathological analysis of cutaneous GVHD. **C:** Histopathological analysis of ear skin from animals with GVHD on days 7, 14, 21, and 40 after transplantation revealed a pattern of sequential alterations that correlated with allostimulation, homing, and targeting stages of disease progression. On day 7 after HSCT (late allostimulation/early homing stage), the skin appeared relatively normal, with the only pathological changes consisting of rare dermal vessels [**top** (**inset**, **arrowhead**)] cuffed by occasional lymphocytes and dermal mast cells containing clear cytoplasmic vacuoles indicating degranulation [**bottom**, **arrow**; compare with fully-granulated mast cell (**inset**, **arrow**) from control animal]. By day 14 (homing/early targeting stage), lymphocytes were diffusely present within the dermis and focally within the epidermal layer in association with early apoptosis (**top**, **arrow**, and at higher magnification at **bottom**). On day 14 and thereafter, the epidermal thickness was twice that observed on day 7 and the superficial epidermis exhibited marked hypergranulosis (**bottom**, **arrow**). By days 21 and 40 (targeting stage), there were multiple foci of epidermal apoptosis (day 21: **top**, **arrows**; day 40: **top** panel to **left** of field; higher magnifications depicted in respective **bottom** panels). Note also that at the day 21 and 40 time points, the entire dermal thickness (**top**) was more than twice that observed on days 7 and 14 after HSCT.

result in significant GVHD morbidity without early mortality. We monitored all recipients weekly for clinical signs of GVHD and detected significantly higher clinical GVHD scores in the recipients of TCD-BM + T cells compared with recipients of TCD-BM only (Figure 1A). Only two GVHD mice (days 21 and 40 after HSCT) showed clinical ear involvement (erythema). The clinical signs of GVHD correlated with histological changes that are associated with the development of murine cutaneous GVHD (Figure 1, B and C). On day 7 after HSCT, the skin appeared relatively normal with the only pathological changes consisting of rare dermal vessels cuffed by occasional lymphocytes and dermal mast cells containing clear cytoplasmic vacuoles indicating degranulation. By day 14, lymphocytes were diffusely present within the dermis and focally within the epidermal layer in association with early keratinocyte apoptosis. On day 14 and thereafter, the epidermal thickness exceeded twice that observed on day 7 and the superficial epidermis exhibited marked hypergranulosis. By days 21 and 40 after HSCT, there were multiple foci of epidermal apoptosis and the entire dermal thickness was more than twice that observed on days 7 and 14.

Gene Expression Overview and Quality

On days 7, 14, 21, and 40 after HSCT, we isolated RNA for DNA microarray analysis from the ear skin of four GVHD mice and four control mice (except day 40 control group: three mice). Unsupervised hierarchical clustering (by correlation) was used to assess grouping of the bio-

logical replicates. This approach grouped the GVHD replicate mice and the control replicate mice on days 7, 14, and 40 after HSCT, indicating a clear difference in the overall cutaneous gene expression profile between GVHD and control mice. Of 141 genes up-regulated in GVHD in a pilot study (42 days after HSCT; GVHD = 4, control = 3), 106 (75%) were also up-regulated in the kinetic study (40 days after HSCT; GVHD = 4, control = 3), indicating considerable reproducibility of the model and methods. The number of differentially expressed genes (GVHD *versus* control) was at least 3.94 times the number anticipated by chance alone. In groups predicted to have identical gene expression profiles [control mice 42 days after HSCT (n = 3) and control mice 40 days after HSCT (n = 3)], the number of differentially expressed genes (n = 351) was essentially the same as the number anticipated by chance alone (n = 361), thereby validating the statistical approach. Of 12,488 genes on the array, 314, 630, 350, and 484 were up-regulated and 312, 793, 293, and 449 were down-regulated in the GVHD group on days 7, 14, 21, and 40 after HSCT, respectively. Complete gene expression data are available in a searchable database at *http://www.amjpathol.org.* The most up-regulated genes in murine cutaneous GVHD are presented in Table 1 and the most down-regulated genes are presented in Table 2.

Effector Cell Markers

Gene expression data for effector cell markers are presented in Figure 2. Mast cell protease 7 stimulates eosinophil accumulation *in vivo*[7] and was up-regulated on days 7 and 14 after HSCT, with expression levels approaching control by day 40 after HSCT. Expression of both CD8-α and CD8-β was up-regulated modestly in murine cutaneous GVHD, although the mean signal for both transcripts did not exceed the limit of detection. In contrast, CTLA-2α (expressed on activated cytotoxic T cells and mast cells[8]) was up-regulated significantly on day 7 after HSCT, with expression levels declining steadily throughout the course of the study. The expression of CD3 epsilon and CD4, which are important for T-cell receptor signaling and T-cell co-stimulation, respectively, was increased throughout the development of cutaneous GVHD and peaked on day 14 after HSCT, whereas CD8 expression peaked early on day 7 (Table 1). Macrosialin (CD68), a sialomucin transmembrane glycoprotein found in tissue macrophages and to a lesser extent in dendritic cells,[9] was up-regulated significantly on day 14 after HSCT and thereafter. The expression of the glycoprotein receptor 49A, which is present on the cell surface of subsets of natural killer (NK) and NK-T cells,[10,11] peaked on day 14 after HSCT and remained above control levels for the remainder of the study.

Chemokines and Their Receptors

Gene expression data for chemokines and their receptors are presented in Figure 3. Many chemokines were highly up-regulated in murine cutaneous GVHD on day 7 after HSCT including CXCL-1, CXCL-9 (MIG), CXCL-10 (IP-10), CCL-2 (MCP-1), CCL-6, CCL-7 (MCP-3), CCL-8 (MCP-2), CCL-9 (MIP-1γ), CCL-11 (eotaxin, Scya11), and CCL-19. Of these, CXCL-1, CCL-2 (MCP-1), CCL-7 (MCP-3), CCL-11 (eotaxin, Scya11), and CCL-19 expression levels decreased throughout the course of the study. Expression of the mast cell-specific CCR1 chemokine receptor peaked on day 14 after HSCT, coincident with peak expression of mast cell protease 7 (Figure 2). Expression levels of CCL-5 (RANTES), which is primarily produced by activated T cells, and CCR5 (one of three RANTES receptors) were up-regulated on day 14 after HSCT, coincident with peak expression of T-cell markers CD3-ϵ and CD4 (Figure 2). The kinetics of CCL-5 gene expression correlated with that of CCL-5 protein expression as determined by ELISA of homogenized ear skin samples (Figure 4). S100A8 (MRP8) expression was up-regulated in murine cutaneous GVHD from day 7 onwards. Peak expression of the complement C3 chemoattractant on day 7 after HSCT was followed on day 14 by peak expression of the C3aR1 complement receptor.

Adhesion Molecules and Their Ligands

Gene expression data for adhesion molecules and their ligands are presented in Figure 5. Expression of the α_M (CD11b), β_2 (CD18), β_7, α_X (CD11c) integrins, PSGL-1 (CD162), Ly9, and ninjurin 1 were all up-regulated during the development of cutaneous GVHD from day 14 after HSCT. Expression of ICAM-1 (CD54), CD2, and the ancillary transforming growth factor (TGF)-β receptor endoglin (CD105) was up-regulated on day 7 after HSCT with expression decreasing throughout the course of the study. VCAM-1 (CD106) expression was up-regulated throughout the study.

Antigen Processing and Presentation

Gene expression data for antigen-processing and presentation molecules are presented in Figure 6. MHC class I expression was up-regulated significantly on day 7 after HSCT but declined steadily throughout the course of the study. Conversely, MHC class II expression was up-regulated significantly on day 14 after HSCT and thereafter. The expression of the co-stimulatory receptor CD80 (B7-1),[12] which is found on antigen-presenting cells such as dendritic cells, monocytes/macrophages, and B cells, was up-regulated throughout the study. Various proteasome (Psm) subunits were up-regulated throughout the study, as were transporters associated with antigen processing 1 and 2 (TAP1 and TAP2). The proteasome generates peptides that are translocated by TAP1 and TAP2 to the endoplasmic reticulum, where they associate with MHC class I molecules for export to the cell surface.

Regulators of Apoptosis

The presence of apoptotic keratinocytes is a prominent feature of acute cutaneous GVHD as we have described previously.[13,14] Gene expression data for apoptosis reg-

Table 1. Up-Regulated Gene Expression in Murine Cutaneous GVHD

Day 7 after HSCT	-Fold	Day 14 after HSCT	-Fold	Day 21 after HSCT	-Fold	Day 40 after HSCT	-Fold
Serum amyloid A 3	199.4	CCL5 (RANTES)	181.5	Serum amyloid A 3	27.2	CCL5 (RANTES)	183
CxCL9 (MIG)	79.7	Serum amyloid A 3	61.8	CCL5 (RANTES)	13.5	Serum amyloid A 3	84.5
CxCL10 (IP-10)	32.6	Small proline-rich protein 2C	27	TCR α chain	11.6	GenBank AA689670	32.4
CCL5 (RANTES)	29.8	Granzyme B	17.6	Macrophage C-type lectin	9.1	Eosinophil chemotactic cytokine ECF-L	31.2
Ubiquitin D	22	Zeta-chain (TCR) associated protein kinase zap-70	17.3	TCR zeta-chain associated protein kinase zap-70	7.3	Interleukin-1 beta	24.3
TCR-α chain	20.2	Migration inhibitory factor-related protein 8 (MRP8)	16.5	CSF/IL3 cytokine receptor common beta chain	6.9	CxCL9 (MIG)	21.9
Interferon-activated gene 205	20.1	GenBank AA689670	14.6	Immune-responsive protein 1	5	Small proline-rich protein 2E	21.6
Lipocalin 2	18.7	GenBank AA958903	14.5	GenBank AA958903	5	Migration inhibitory factor-related protein 8	21.5
Interferon-induced protein with tetratricopeptide repeats 1	15	Migration inhibitory factor-related protein 8 (MRP8)	12.5	CCL9 (MIP-1 gamma)	4.9	Protease, serine, 18	20.7
CD2	14.9	Interleukin-1 beta	12.1	Eosinophil chemotactic cytokine ECF-L	4.7	Keratin 16	20
GenBank AA689670	12	Lipocalin 2	12.1	Major urinary protein 2	4.5	Repetin	18.9
GenBank AA958903	11.8	MMP-12	11.3	MMP-12	4.3	Migration inhibitory factor-related protein 14	17.2
Interferon-induced GTP binding protein Mx1	11.8	CSF/IL3 cytokine receptor common beta chain	10.3	Granzyme B	4.1	Small proline-rich protein 1B	15.3
CCL17 (TARC)	11.1	Eosinophil chemotactic cytokine ECF-L	10	Lysozyme c, type p	3.7	Keratin 5	14
Guanylate nucleotide-binding protein 2	10.6	Keratin 16	9.3	Platelet-activating factor acetylhydrolase	3.7	Guanylate nucleotide binding protein 2	13.2
Migration inhibitor factor-related protein 8 (MRP8)	10.6	Keratin 5	9	Lymphotoxin-beta	3.6	Immune-responsive protein 1	13
GenBank AV152244	10.3	Small proline-rich protein 1B	8.5	Neutrophil cytosol factor 1	3.6	CSF/IL3 cytokine receptor common beta chain	12.9
Bcl-3	9.8	Macrophage C-type lectin	8.5	Lymphocyte-specific protein tyrosine kinase	3.6	Elafin-like protein II	12.7
Ubiquitin-specific protease 18	9.6	CxCL9 (MIG)	8.5	CD64 (IgG high-affinity Fc receptor)	3.5	CxCL10 (IP-10)	11.6
CCL2 (MCP-1)	9.5	Immune-responsive protein 1	8.3	Lymphocyte antigen 9 (Ly-9)	3.4	Macrophage C-type lectin	10.9
Keratin 16	9.3	CD18 (integrin β2)	8.2	MMP-12	3.4	Keratin 6	10.5
Interferon-gamma-inducible protein, 47 kd	9.1	CD3 epsilon	8.1	Cytochrome b-245, beta polypeptide	3.3	CxCL2 (MIP-2)	10.1
Onzin	8.8	Platelet-activating factor acetylhydrolase	8.1	Lymphocyte cytosolic protein 2	3.3	GCSFR	9.9
CD8 β opposite strand	8.8	G-CSFR	7.5	Interferon-activated gene 205	3.3	T-cell-specific GTPase	9.5
Protein tyrosine phosphatase 70z-pep	8.7	MMP-12	7.5	Complement C1q B	3.3	Immunoglobulin kappa chain variable 28	9.3

Fold changes were calculated by dividing the mean signal in the GVHD group by the mean signal in the control group. Shown are 25 genes with the most up-regulated expression in GVHD on each day (7, 14, 21, or 40) after HSCT. Genes not characterized functionally are identified by GenBank numbers. Because Affymetrix microarrays occasionally use two separate probe sets to assess gene expression level, some genes are listed twice on a single day after HSCT.

Table 2. Down-Regulated Gene Expression in Murine Cutaneous GVHD

Day 7 after HSCT	-Fold	Day 14 after HSCT	-Fold	Day 21 after HSCT	-Fold	Day 40 after HSCT	-Fold
Long chain fatty acyl elongase	5.3	Carboxylesterase 3	25.4	Long chain fatty acyl elongase	3.7	Carboxylesterase 3	8.5
Tyrosinase-related protein 1	5.2	Carboxylesterase 3	9.3	Monoglyceride lipase	3.2	Carboxylesterase 3	6.8
Alpha-1 type I procollagen	4.6	Carbonic anhydrase 3	5.1	Cell death-inducing DNA fragmentation factor, alpha subunit-like effector A	3.2	Long chain fatty acyl elongase	5.1
Long chain fatty acyl elongase	4.5	GenBank AW122078	5.0	Alpha-1 type VIII procollagen	2.5	Slow myosin heavy chain-beta	4.4
Alpha-1 type III procollagen	4.5	Myosin heavy chain 2B	5.0	Eosinophil-associated ribonuclease 3	2.5	GenBank AW124134	4.2
Alpha-1 type I procollagen	4.4	ATPase, Ca++ transporting, cardiac muscle, fast twitch 1	4.8	Chondroadherin	2.5	Long chain fatty acyl elongase	3.9
Type III collagen	4.0	Insulin-like growth factor binding protein 6	4.8	Serine (or cysteine) proteinase inhibitor, clade F), member 1	2.5	Cell death-inducing DNA fragmentation factor, alpha subunit-like effector A	3.9
Dopachrome tautomerase	3.9	Plexin B2	4.8	Insulin-like growth factor binding protein 6	2.5	GenBank AI842353	3.9
Secreted frizzled-related sequence protein 2	3.7	Retinol-binding protein	4.4	GenBank AI842353	2.4	GenBank AI834895	3.7
Hemoglobin, beta adult major chain	3.6	Dermatopontin	4.1	Long chain fatty acyl elongase	2.4	Insulin-like growth factor-binding protein 3	3.6
D site albumin promoter binding protein	3.5	GenBank AI645694	4.1	Osteoglycin	2.3	Myosin alkali light chain (exon 1)	3.6
Alpha-2 type I procollagen	3.5	Phosphoglycerate mutase 2	4.0	Fibromodulin	2.3	Cysteine-rich protein 3	3.3
Neuronal protein 3.1	3.5	Troponin T3, skeletal, fast	3.9	Sterol-C4-methyl oxidase-like	2.2	Monoglyceride lipase	3.2
Hemoglobin, beta adult minor chain	3.3	Neuronal guanine nucleotide exchange factor	3.9	GenBank AA690483	2.2	Dermatopontin	3.2
Silver	3.1	Muscle glycogen phosphorylase	3.8	Glutathione *S*-transferase, mu 5	2.2	Carbonic anhydrase 3	3.2
Hemoglobin alpha, adult chain 1	3.1	Creatine kinase, mitochondrial 2	3.8	Aminolevulinate, delta-, dehydratase	2.1	Four and a half LIM domains 1	3.1
Immunoglobulin kappa light chain variable region	2.9	Thyroid hormone-responsive SPOT14 homolog	3.8	Ephrin B2	2.1	Mesoderm posterior 2	3.1
GenBank AI853444	2.9	Troponin C, fast skeletal	3.8	Cytochrome P450, 2b19	2.1	Myosin light chain, phosphorylatable, cardiac ventricles	3.0
Stearoyl-CoA desaturase	2.9	Long chain fatty acyl elongase	3.7	GenBank AA873956	2.1	Serine (or cysteine) proteinase inhibitor, clade F), member 1	3.0
Cell death-inducing DNA fragmentation factor, alpha subunit-like effector A	2.9	Carboxypeptidase X 2 (M14 family)	3.7	S100 calcium-binding protein A3	2.1	Troponin T1, skeletal, slow	3.0
Metallothionein 4	2.9	GenBank AI019679	3.5	Carboxypeptidase X 2 (M14 family)	2.0	GenBank AI842065	3.0
Glutathione *S*-transferase, alpha 2 (Yc2)	2.8	Phosphofructokinase, muscle	3.4	Myocilin	2.0	Troponin T3, skeletal, fast	2.9
Osteoblast specific factor 2 (fasciclin I-like)	2.7	Fatty acid synthase	3.4	Cytokine receptor-like factor 1	2.0	GenBank AI413993	2.9
Monoglyceride lipase	2.7	Long chain fatty acyl elongase	3.4	GenBank AW125453	2.0	Similar to orphan nuclear receptor NR1D1 (V-erbA related protein EAR-1) (Rev-erbA-alpha)	2.8
Alpha-1 type V procollagen	2.7	GenBank AI847230	3.3	GenBank AV321418	2.0	Sciellin	2.7

Fold changes were calculated by dividing the mean signal in the control group by the mean signal in the GVHD group. Shown are 25 genes with the most down-regulated expression in GVHD on each day (7, 14, 21, or 40) after HSCT. Genes not characterized functionally are identified by GenBank numbers. Because Affymetrix microarrays occasionally use two separate probe sets to assess gene expression level, some genes are listed twice on a single day after HSCT.

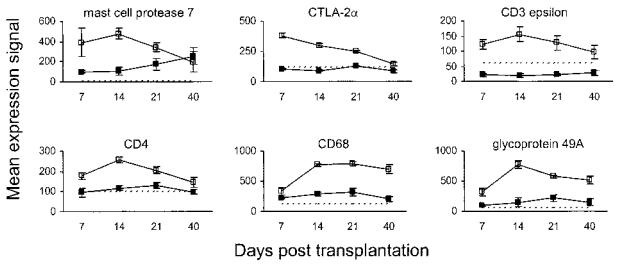

Figure 2. Kinetics of effector cell gene expression in murine cutaneous GVHD. Mice were transplanted as described in Figure 1. On days 7, 14, 21, and 40 after transplantation, four mice per group were sacrificed (except day 40 control group: three mice) and RNA was obtained from ear skin. Data shown are mean gene expression signals (±SE) in GVHD (**open squares**) and control (**closed squares**) groups. The **dotted line** represents the mean gene expression signal in untreated CBA/J mice ($n = 4$).

ulators are presented in Figure 7. Granzyme B expression in murine cutaneous GVHD peaked on day 14 after HSCT and returned toward control levels thereafter. Granzyme B is a serine protease used by CTLs and NK cells to induce apoptosis in target cells, which has a significant role in GVHD mediated by $CD8^+$ T cells.[15] The expression of lymphotoxin B and caspases 1 and 11 was up-regulated throughout the study. Lymphotoxin B is primarily involved in the organogenesis of lymphoid tissues.[16] Caspase 1 (interleukin-1β-converting enzyme) is essential for the induction of interleukin (IL)-1α, IL-1β, and IL-18 by lipopolysaccharide.[17] Caspase 11 is related to caspase 1 and is also activated during inflammation.[17] The expression of caspases 7 and 14 was up-regulated in the latter half of the study. Caspase 7 is a downstream effector caspase.[17] Caspase 14 is expressed in the epidermis, choroid plexus, retinal pigment epithelium, and thymic Hassall's bodies, although its function is unknown.[18] Proapoptotic members of the *Bcl*II family [Bak1,

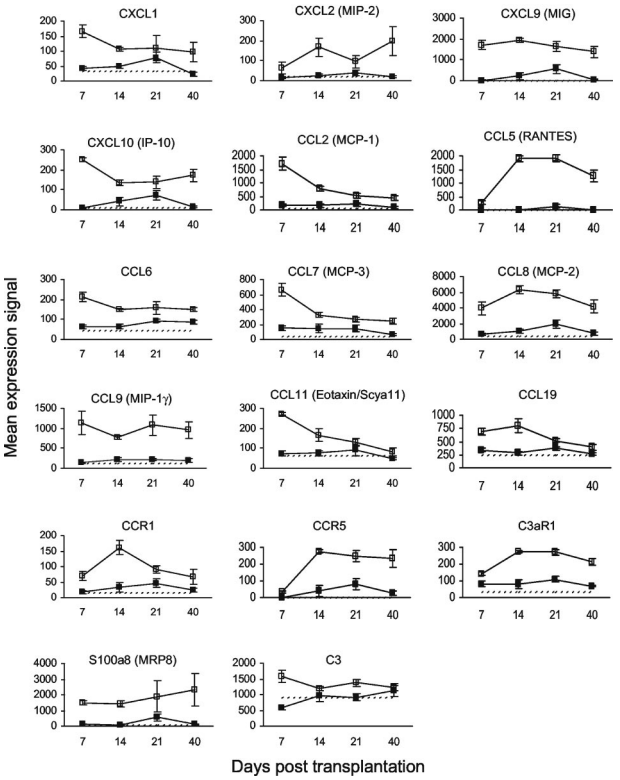

Figure 3. Kinetics of gene expression for chemokines and their receptors in murine cutaneous GVHD. Mice were transplanted as described in Figure 1. On days 7, 14, 21, and 40 after transplantation, four mice per group were sacrificed (except day 40 control group: three mice) and RNA was obtained from ear skin. Data shown are mean gene expression signals (±SE) in GVHD (**open squares**) and control (**closed squares**) groups. The **dotted line** represents the mean gene expression signal in untreated CBA/J mice ($n = 4$).

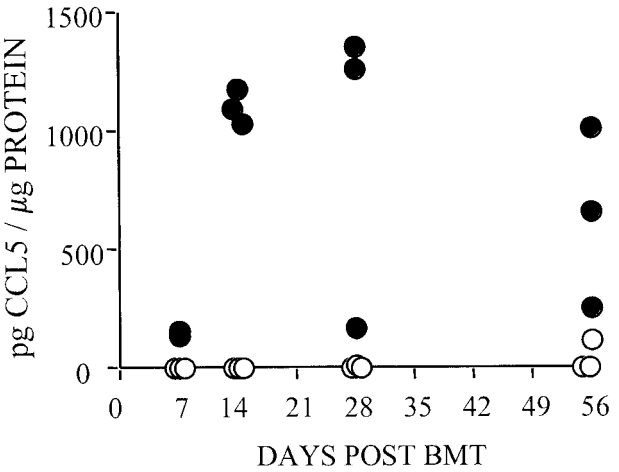

Figure 4. Kinetics of CCL-5 (RANTES) protein concentration in murine cutaneous GVHD. Mice were transplanted as described in Figure 1. On days 7, 14, 28, and 56 after transplantation, three mice per group were sacrificed and ear skin was harvested and homogenized. Data shown are CCL-5 concentrations (pg CCL-5/μg total protein) in ear skin homogenates as determined by ELISA from individual GVHD (**filled circle**) and control (**open circle**) mice.

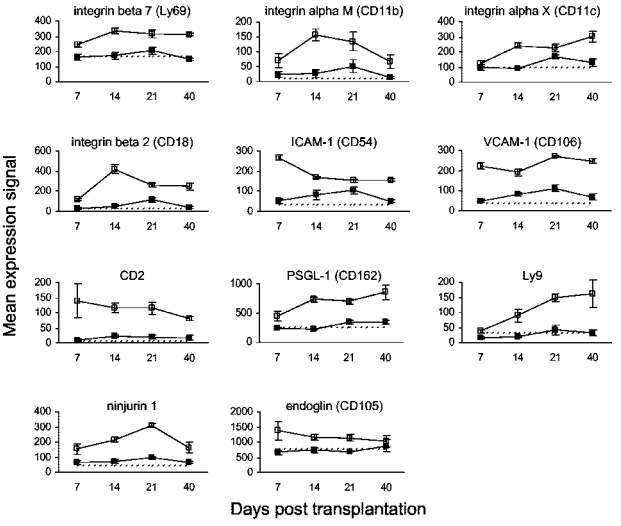

Figure 5. Kinetics of gene expression for adhesion molecules and their ligands in murine cutaneous GVHD. Mice were transplanted as described in Figure 1. On days 7, 14, 21, and 40 after transplantation, four mice per group were sacrificed (except day 40 control group: three mice) and RNA was obtained from ear skin. Data shown are mean gene expression signals (±SE) in GVHD (**open squares**) and control (**closed squares**) groups. The **dotted line** represents the mean gene expression signal in untreated CBA/J mice ($n = 4$).

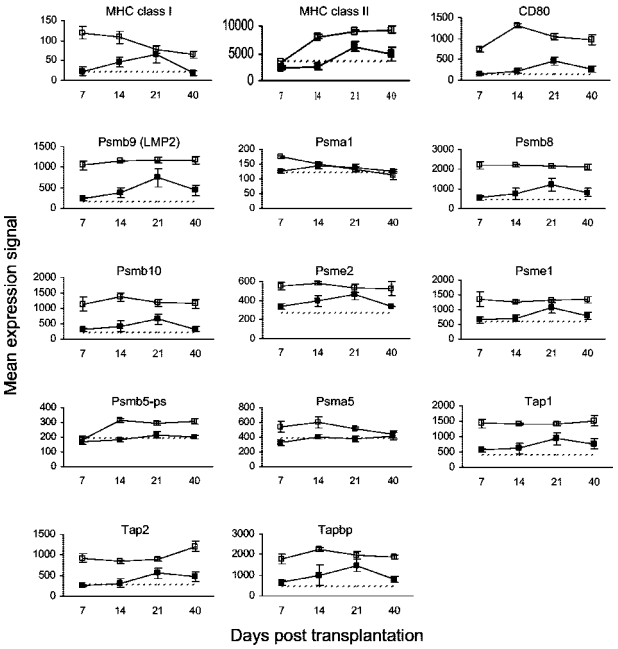

Figure 6. Kinetics of gene expression for molecules involved in antigen processing and presentation in murine cutaneous GVHD. Mice were transplanted as described in Figure 1. On days 7, 14, 21, and 40 after transplantation, four mice per group were sacrificed (except day 40 control group: three mice) and RNA was obtained from ear skin. Data shown are mean gene expression signals (±SE) in GVHD (**open squares**) and control (**closed squares**) groups. The **dotted line** represents the mean gene expression signal in untreated CBA/J mice ($n = 4$).

Bcl2l11 (Bim), Bax][19] were up-regulated from day 14 onwards. Expression of *Bcl*II and *Bcl*III, which inhibit B- and T-cell apoptosis,[20,21] was up-regulated throughout the study.

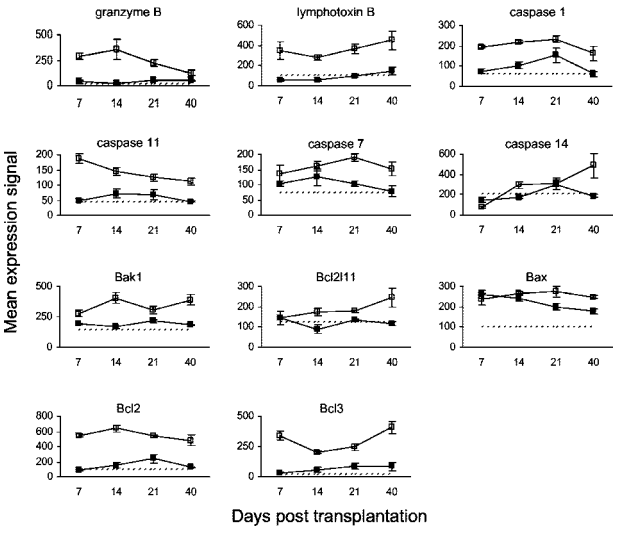

Figure 7. Kinetics of gene expression for molecules involved in the regulation of apoptosis in murine cutaneous GVHD. Mice were transplanted as described in Figure 1. On days 7, 14, 21, and 40 after transplantation, four mice per group were sacrificed (except day 40 control group: three mice) and RNA was obtained from ear skin. Data shown are mean gene expression signals (±SE) in GVHD (**open squares**) and control (**closed squares**) groups. The **dotted line** represents the mean gene expression signal in untreated CBA/J mice ($n = 4$).

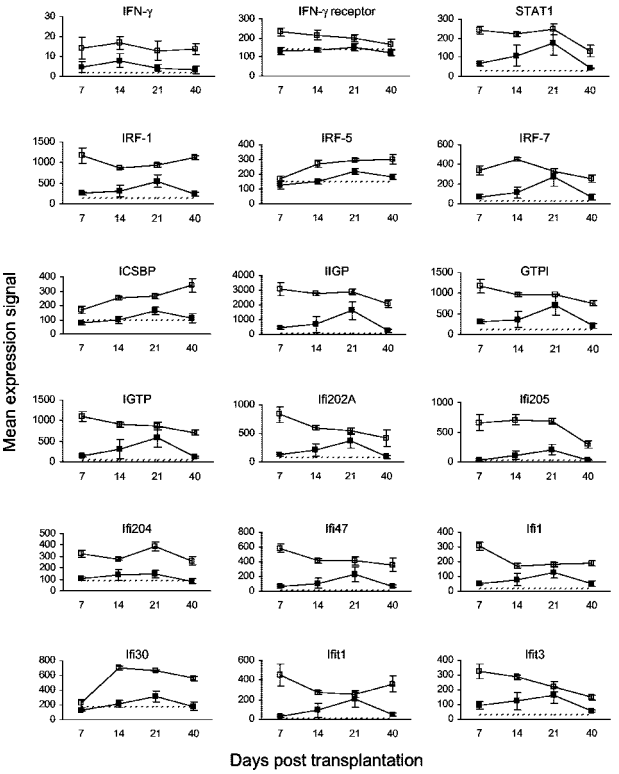

Figure 8. Kinetics of gene expression for molecules inducible by IFN-γ in murine cutaneous GVHD. Mice were transplanted as described in Figure 1. On days 7, 14, 21, and 40 after transplantation, four mice per group were sacrificed (except day 40 control group: three mice) and RNA was obtained from ear skin. Data shown are mean gene expression signals (±SE) in GVHD (**open squares**) and control (**closed squares**) groups. The **dotted line** represents the mean gene expression signal in untreated CBA/J mice ($n = 4$). The apparent up-regulation of IFN-γ expression was not statistically significant because mean expression in both GVHD and control groups was below the limit of detection.

Inducible by Interferon (IFN)-γ

Although IFN-γ expression was not up-regulated, the IFN-γ receptor and many genes associated with IFN-γ stimulation were up-regulated significantly in the early phase (days 7 and 14) of murine cutaneous GVHD (Figure 8). The expression of signal transducer and activator of transcription-1 (STAT1), which translocates to the nucleus after phosphorylation of the IFN-γ receptor and stimulates the expression of various transcription factors including interferon regulatory factors (IRF) and IFN consensus sequence binding protein (ICSBP), remained elevated on days 7, 14, and 21.[22] Other up-regulated genes include IFN-inducible GTPases (IIGP, GTPI, IGTP), IFN-activated genes (Ifi202A, Ifi205, Ifi204, Ifi47, Ifi1, Ifi30), and IFN-induced proteins with tetratricopeptide repeats (Ifit1, Ifit3).[22,23]

Keratinocyte Proliferation and Differentiation, Dermal Fibrosis, and Acute-Phase Proteins

Gene expression data relevant to keratinocyte proliferation and differentiation, dermal fibrosis, and acute-phase proteins are presented in Figure 9 and Table 1. Keratin 5 (present in basal keratinocytes in the epidermis[24]) and

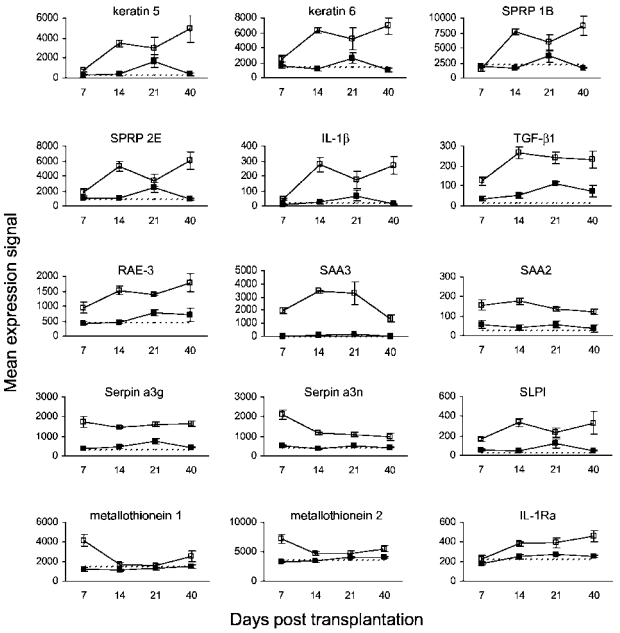

Figure 9. Kinetics of gene expression related to keratinocyte proliferation and differentiation, dermal fibrosis, and acute-phase proteins in murine cutaneous GVHD. Mice were transplanted as described in Figure 1. On days 7, 14, 21, and 40 after transplantation, four mice per group were sacrificed (except day 40 control group: three mice) and RNA was obtained from ear skin. Data shown are mean gene expression signals (±SE) in GVHD (**open squares**) and control (**closed squares**) groups. The **dotted line** represents the mean gene expression signal in untreated CBA/J mice ($n = 4$).

keratin 6 (expressed during wound healing in skin appendages[24,25]) were up-regulated in murine cutaneous GVHD from day 14 after HSCT onwards. The expression of small proline-rich proteins 1B and 2E, which can function as cross-bridges in the cornified cell envelope of stratified squamous epithelia,[26] followed a similar pattern. Expression of IL-1β (an inflammatory cytokine with many other effects[27]) and TGF-β1, which has anti-inflammatory and profibrotic effects,[28] was also increased from day 14 onwards. RAE-3 expression (a potential ligand for the activating NK receptor NKG2D[29]) increased during the development of cutaneous GVHD. One of the most up-regulated genes at all time points was the acute-phase protein serum amyloid A3 (SAA3). Other up-regulated acute-phase proteins include SAA2, serpins a3g and a3n, secretory leukocyte protease inhibitor (SLPI), metallothioneins 1 and 2, and IL-1 receptor antagonist (IL-1Ra).

Discussion

We used microarray gene expression analysis (see *http://www.amjpathol.org.* for complete data on 12,488 genes) of whole tissues to associate the kinetics of gene expression with the development of murine cutaneous GVHD. At the transcriptional level, these data shed light on the development and composition of the mononuclear infiltrate, the triggers of keratinocyte apoptosis, and the mechanisms underlying epithelial hyperplasia and dermal fibrosis in murine cutaneous GVHD.

Few studies have used cDNA microarray technology to analyze kinetic profiles of gene expression in whole tissues. The pattern of chemokines with increased expression in the current study primarily overlaps that described by Mitsui and colleagues[30] during contact hypersensitivity in mice and includes CCL-2, CCL-7, CCL-9, CCL-19, CXCL-1, CXCL-9, and CXCL-10. Mitsui and colleagues[30] observed up-regulated expression of these chemokines within hours of ear challenge with 2,4,6-trinitrochlorobenzene. Consistent with these findings, the same chemokines were up-regulated at the earliest time point (day 7) in the current murine cutaneous GVHD study. Mitsui and colleagues[30] also observed up-regulated IFN-γ expression within hours of ear challenge. In contrast, cutaneous IFN-γ expression was not up-regulated at any of the observed time points in the current study. These data are consistent with the hypothesis that IFN-γ production occurs at sites of antigenic challenge—the skin in contact hypersensitivity and possibly the secondary lymphoid organs in GVHD, as discussed below. Ichiba and colleagues[31] examined gene expression during the development of murine hepatic GVHD in the B6 → irradiated B6D2F1 transplantation model. As shown in the liver, we found evidence in murine cutaneous GVHD for early expression of a variety of chemokines (CXCL-1, CXCL-9, CXCL-10, CCL-2, CCL-5, CCL-7), adhesion molecules (ICAM-1, VCAM-1, CD18), antigen processing and presentation molecules (LMP2, TAP1, TAP2, MHC class II), IFN-inducible genes (STAT1, IRF-1, IRF-7, ICSBP, IIGP, GTPI, Ifi202A, Ifi204, Ifit1, Ifit3), and acute-phase proteins (SAA3, serpin a3g, SLPI, metallothioneins 1 and 2, IL-1Ra). Similar to the findings in hepatic GVHD,[31] cutaneous expression of IFN-γ was not up-regulated in the current investigation, suggesting local release of preformed IFN-γ or endocrine IFN-γ activity in murine cutaneous GVHD. The data from Ichiba and colleagues[31] and the current study support the hypothesis that IFN-γ is produced outside of the target organs in murine GVHD and functions in an endocrine manner to up-regulate IFN-inducible gene expression in the liver and skin. As shown by Ichiba and colleagues[31] and Baker and colleagues,[32] the spleen may be the origin of IFN-γ in these models.

Several studies have demonstrated increased secretion of IFN-γ in the first phase of the development of GVHD with peak serum levels on day 7.[32–35] IFN-γ is an important type II cytokine in the Th1/Tc1 response and is primarily secreted by activated T and NK cells.[22] IFN-γ may contribute in several ways to the pathophysiology of cutaneous GVHD, including 1) stimulation of antigen presentation through up-regulation of MHC class I and II molecules and molecules involved in antigen processing (such as proteasomes and TAP proteins) and co-stimulation; 2) induction of a Th1/Tc1 immune response and IL-12 secretion by monocytes/macrophages; 3) activation of macrophages including release of incompletely reduced oxygen intermediates and nitric oxides; and 4) stimulation of leukocyte-endothelial interactions through the induction of chemokine secretion [such as CXCL-10 (IP-10), CCL-3 (MIP-1α), CCL-4 (MIP-1β), CCL-5 (RANTES), and CCL-2 (MCP-1)] and adhesion molecule

expression (such as ICAM-1 and VCAM-1).[22] In addition, IFN-γ can induce the expression of members of the complement system and the acute-phase response, as discussed below.

A recent study by Zhang and colleagues[36] used a murine model for sclerodermatous GVHD (B10.D2 BM and splenocytes → lethally irradiated BALB/c), which resembles chronic GVHD, and analyzed cutaneous expression patterns of a select group of chemokines, cytokines, and effector cell markers. Similar to our data, they found evidence of early infiltration of donor T cells and monocytes/macrophages, and up-regulation of MHC, chemokine (MCP-1, MIP-1α, RANTES), and TGF-β1 expression. Moreover, anti-TGF-β antibody treatment of the recipients inhibited the infiltration of effector cells, collagen synthesis, and the development of sclerodermatous GVHD. New and colleagues[37] studied the expression patterns from days 1 to 21 of five chemokines by real-time polymerase chain reaction and ELISA in several GVHD target organs in an acute GVHD model without recipient conditioning (B6 splenocytes → CB-17 SCID mice). They found similar expression profiles for CCL-2 and CCL-7 (early peak on day 7) and CXCL-2 (increasing levels throughout time) as in our study.

It is of considerable interest to determine whether the gene expression data correlate with the histopathological evolution of lesions in target tissue (see Figure 1). A three-stage model for the immunopathogenesis of mHAg-induced murine cutaneous GVHD has recently been proposed.[13] During the initial stage, allostimulation, which encompasses the first week after transplantation, only evidence of mast cell degranulation and rare foci of dermal perivascular lymphocyte accumulation are noted.[38] The second stage, homing, involves the second week during which there is progressive lymphocyte accumulation within the dermis and epidermis. Finally in the third stage that follows, targeting, apoptosis is progressively documented within the epidermis and hair follicles.[14] In the current study, as early as day 7 after HSCT, the dermal mast cells contained clear cytoplasmic vacuoles indicating degranulation. In the gene expression study, mast cell markers (eg, mast cell protease 7) and the CCR1 mast cell-specific chemokine receptor were up-regulated in murine cutaneous GVHD on day 14 after HSCT. Early mast cell degranulation, and related biosynthetic activation inherent to regranulation, has been shown to occur in murine acute cutaneous GVHD.[38] In this and other settings, mast cell secretion appears to represent an early trigger whereby dermal vessels become primed for T-cell homing.[39] This effect is believed to result from liberation of preformed mediators (vasoactive peptides, proteases, and cytokines) in the immediate vicinity of dermal microvessels.[40–43] Mast cell mediator release results in endothelial expression of adhesion molecules such as selectins, ICAM-1, and VCAM-1 that bind circulating leukocytes.[40,41] Consistent with previous observations, we found increased expression of adhesion molecules such as ICAM-1 and VCAM-1 as early as day 7 after HSCT.

The formation of the lymphocytic infiltrate requires the expression of various chemokines and adhesion molecules in the developing cutaneous GVHD lesion. The expression of many T-cell chemokines including CXCL-9 (MIG), CXCL-10 (IP-10), CCL-2 (MCP-1), CCL-5 (RANTES), CCL-7, CCL-9 (MIP-1γ), and CCL-11 (eotaxin) was highly up-regulated from day 7. Most of these chemokines are associated with inflammation and are induced by tumor necrosis factor and IFN-γ.[44,45] Of note, CCR5 (a receptor for RANTES and MCP-2) expression, which is associated with Th1 lymphocytes,[46] was up-regulated significantly from day 14 after HSCT. CXCL-9 (MIG) plays a role in the infiltration of activated $CD4^+$ T cells into a skin allograft and anti-CXCL-9 neutralizing antibodies can prevent skin graft rejection.[47] S100A8 (MRP8) and complement C3 were up-regulated in murine cutaneous GVHD on day 7 after HSCT. S100A8 (MRP8) is a small calcium-binding protein that is highly expressed in neutrophils and monocytes during inflammation and promotes neutrophil chemotaxis.[48] As shown in the C57BL/6 → B10.BR kidney transplant model, IFN-γ stimulates complement C3 synthesis by proximal tubular epithelial cells, and local production of complement C3 is required for lymphocyte infiltration and T-cell priming during acute renal transplant rejection.[49]

Most chemokines were highly expressed before the appearance of the lymphocytic infiltrate (day 7 after HSCT), suggesting local production by resident skin cells including monocytes/macrophages, fibroblasts, and keratinocytes. The notable exceptions to this rule were CXCL-2 (MIP-2) and CCL-5 (RANTES) whose expression was significantly up-regulated on day 14 after HSCT, co-incident with the appearance of lymphocytes diffusely within the dermis and focally within the epidermis, a phenomenon also observed in murine hepatic GVHD.[31] The stimulus for chemokine up-regulation early (day 7 after HSCT) in murine cutaneous GVHD is unknown. As discussed, most of these chemokines are induced by tumor necrosis factor and IFN-γ.[44,45] Many IFN-inducible proteins were similarly up-regulated on day 7 after HSCT, while IFN-γ itself was not up-regulated. Together, these data support the hypothesis that IFN-γ is produced extracutaneously in murine GVHD and functions in an endocrine manner to up-regulate cutaneous chemokine gene expression early after transplantation.

Expression of various integrins, PSGL-1 (CD162), Ly9, and ninjurin 1 in murine cutaneous GVHD was up-regulated from day 14 after HSCT. The integrins α_M (CD11b) and β_2 (CD18) combine to form the $\alpha_M\beta 2$ integrin (also called complement receptor 3 or Mac-1) expressed on granulocytes, macrophages, dendritic cells, and NK cells. The $\alpha_M\beta 2$ integrin binds C3bi and ICAM-1.[50] The integrin β_7 chain combines with either the α_4 or α_E chain and is involved in lymphocyte migration to the intestines.[51] The integrin α_X chain (CD11c) binds CD18 to form gp150,95 expressed on dendritic cells and intestinal intraepithelial cells.[50,52] PSGL-1 (CD162) is a ligand for P-selectin (CD62P) involved in leukocyte rolling and, more specifically, in the migration of Th1 T cells into inflamed skin.[53,54] Ly9 is a member of the CD2 subgroup of the immunoglobulin supergene family, which is expressed on lymphocytes and hematopoietic precursor cells.[55,56] Ninjurin 1 is a homophilic adhesion molecule

that is widely expressed in adult and embryonic tissues.[57,58]

Expression of ICAM-1 (CD54), VCAM-1 (CD106), CD2, and the ancillary TGF-β receptor endoglin (CD105) was up-regulated in murine cutaneous GVHD on day 7 after HSCT. ICAM-1 (CD54) is a ligand for LFA-1 (CD11a/CD18) and Mac-1 (CD11b/CD18) and is expressed on lymphocytes, vascular endothelium, high endothelial venules, epithelial cells, macrophages, and dendritic cells.[59,60] VCAM-1 (CD106) is expressed on myeloid and endothelial cells and is a receptor for the $\alpha_4\beta7$ and $\alpha_4\beta1$ integrins. The expression of ICAM-1 and VCAM-1 on endothelial cells is up-regulated during inflammation and is important for the migration of leukocytes into sites of inflammation.[61] CD2 is expressed on T lymphocytes and at low levels on NK cells and certain BM B lymphocytes. Interaction between LFA-3 (CD58) on antigen-presenting cells and CD2 on T lymphocytes is involved in T-cell activation.[62,63] The ancillary TGF-β receptor endoglin (CD105) is expressed on endothelial cells and long-term repopulating hematopoietic stem cells[64] and is involved in vasculogenesis and angiogenesis.[65] In previous studies, anti-VCAM-1 and anti-α_4 integrin antibodies reduced the incidence and delayed the onset of murine GVHD.[66,67] Moreover, recent data indicates that VCAM-1 is expressed not only by endothelial cells in murine GVHD, but also by keratinocytes at sites destined for eventual targeting.[68] In the current study, VCAM-1 (CD106) expression was up-regulated in murine cutaneous GVHD from day 7 after HSCT onwards, although α4 integrin (VCAM-1 ligand) was not up-regulated. In contrast, both ICAM-1 (CD54) and its ligand (β2 integrin; CD18) were up-regulated on days 7 and 14 after HSCT, respectively, consistent with a role for ICAM-1 in GVHD.[69,70]

Fourteen days after HSCT, the epidermis doubled in thickness and there was marked hypergranulosis in the superficial epithelium. Consistent with these observations, markers of keratinocyte proliferation (keratins 5 and 6) and differentiation (small proline-rich proteins 2E and 1B) were also up-regulated from day 14. Of interest in this context is that IL-1β and TGF-β followed a similar pattern of expression, while both are known to regulate epidermal differentiation.[71,72] Previous studies documented a high percentage of Ki-67$^+$ epidermal cells, suggesting up-regulated keratinocyte proliferation in cutaneous GVHD.[73] In addition to inhibiting lymphocyte apoptosis during the development of the mononuclear infiltrate,[20,21] up-regulated *Bcl*II and *Bcl*III expression in murine cutaneous GVHD may provide a keratinocyte survival signal, thereby contributing to epidermal thickening. The histopathology of murine cutaneous GVHD was also characterized by increased thickness and sclerosis of the dermis that became evident on day 21 after HSCT. In addition to regulating epithelial differentiation, IL-1β and TGF-β1 stimulate fibroblast proliferation and synthesis of extracellular matrix proteins including type I collagen, elastin, and fibronectin.[74–77] As discussed, IL-1β and TGF-β1 were up-regulated from day 14 after HSCT. Hence, dermal thickening in murine cutaneous GVHD may result from IL-1β and TGF-β1 stimulation of dermal fibroblasts. It is noteworthy that IL-1β and caspase 1 (IL-1β-converting enzyme involved in IL-1β activation) were up-regulated simultaneously in murine cutaneous GVHD.

On day 7 after HSCT, there was considerable down-regulation of α-1 type I procollagen, α-1 type III procollagen, type III collagen, α-2 type I procollagen, and α-1 type V procollagen in murine cutaneous GVHD (Table 2). This phenomenon was evident before the appearance of the lymphocytic infiltrate and before the up-regulation of IL-1β and TGF-β1. As discussed below, SAA3 and other acute-phase proteins were up-regulated profoundly on day 7 after HSCT, suggesting that a stress response in the skin may have shut down collagen synthesis at this early time point. As described for IFN-inducible genes and various chemokines, the stress response on day 7 in murine cutaneous GVHD may be triggered by endocrine IFN-γ. After day 7, local production of IL-1β, TGF-β1, and possibly other profibrotic cytokines may have overridden the initial stress response, resulting in dermal thickening by day 21 after HSCT. As described in murine hepatic GVHD, many genes associated with metabolic function were similarly down-regulated in murine cutaneous GVHD on day 7 after HSCT, probably reflecting the stress response in this tissue.[31]

CTLA-2α (activated cytotoxic T-cell marker), CD8β, TCRα, granzyme B, and lymphotoxin β were up-regulated on day 7 after HSCT, suggesting early infiltration and activation of cytotoxic CD8$^+$ T cells. This is in agreement with the observation that GVHD in this particular model is mediated primarily by CD8$^+$ T cells.[78] On day 14 after HSCT, CD3, CD4, TCR zeta chain, granzyme B, MHC class II, and CD80 expression increased, suggesting subsequent activation and differentiation of Th1 helper T cells. GVHD is thought to be initiated by donor T cells that recognize host mHAgs, whereas NK cells could play an important role in the effector phase of the pathophysiology of cutaneous GVHD.[79] Some mHAgs bind to the activating NKG2D receptor expressed by NK cells and activated CD8$^+$ T cells, $\gamma\delta$ T cells, and macrophages. In mice, NKG2D binds the H60 peptide and members of the retinoic acid early inducible (RAE) family of molecules.[80,81] In the current study, glycoprotein 49A (NK cell marker) and RAE-3 expression increased by day 14 after HSCT, coincident with decreasing expression of MHC class I (an inhibitor of NK cell activity) through an unknown mechanism. These data could suggest that, after an initial wave of cytotoxic T-cell activity, keratinocyte apoptosis may be triggered by granzyme B produced by RAE-activated NK cells.[79,82] Other triggers of apoptosis (tumor necrosis factor-α, p55 tumor necrosis factor receptor, FasL, Fas) were not up-regulated in the current study, consistent with the finding that host Fas deficiency does not alleviate murine cutaneous GVHD.[83] In contrast, Fas expression was up-regulated in murine hepatic GVHD on day 7 after transplantation, consistent with a role for Fas-mediated T-cell cytotoxicity in the development of hepatic GVHD.[31]

One of the most up-regulated genes at all time points was serum amyloid A3 (SAA3). SAA is a 12,500 d acute-phase protein produced primarily by hepatocytes. Amy-

loid A (AA) is the 7500 d cleavage product of SAA that accumulates in various tissues in AA amyloidosis associated with chronic inflammatory diseases. SAA is also produced extrahepatically during inflammation by epithelial and adipose tissue, smooth muscle, endothelial cells, and macrophages. SAA is involved in the suppression of the immune response, inhibition of platelet aggregation, detoxification of endotoxin, migration of monocytes, polymorphonuclear leukocytes and T cells, and inhibition of the neutrophil oxidative burst.[84,85] SAA binds the FPRL1 (LXA_4R, ALXR) G protein-coupled receptor that also serves as a receptor for lipoxin A_4 (LXA_4).[86] LXA_4 is a potent anti-inflammatory eicosanoid that requires 5-lipoxygenase for its biosynthesis. Ligation between LXA_4 and its receptor inhibits the production of many proinflammatory cytokines including IL-6, IL-8, IL-12, IFN-γ, and MMP-3 via inhibition of the NF-κB pathway.[87–90] Hence, in murine cutaneous GVHD, blockade of the LXA_4 receptor by SAA3 may inhibit LXA_4-mediated anti-inflammatory activity. Furthermore, SAA3 was highly up-regulated in murine cutaneous GVHD before the appearance of the lymphocytic infiltrate, suggesting that SAA3 expression may be stimulated (at least initially) by IFN-γ in an endocrine manner, as described for IFN-inducible genes and various chemokines.

In conclusion, the data suggest early infiltration and activation of cytotoxic $CD8^+$ T and mast cells, followed by $CD4^+$ T, NK, and myeloid cells in this experimental model of cutaneous GVHD. The sequential infiltration and activation of effector cells correlates with the histopathological development of cutaneous GVHD and is accompanied by the up-regulated expression of many chemokines and their receptors (CXCL-1, -2, -9, and -10; CCL-2, -5, -6, -7, -8, -9, -11, and -19; CCR1 and CCR5), adhesion molecules (ICAM-1, CD18, Ly69, PSGL-1, VCAM-1), molecules involved in antigen processing and presentation (TAP1 and TAP2, MHC class I and II, CD80), regulators of apoptosis (granzyme B, caspase 7, Bak1, Bax, and *Bcl*II), IFN-inducible genes (STAT1, IRF-1, IIGP, GTPI, IGTP, Ifi202A), acute-phase proteins (SAA3, serpin, SLPI, metallothionein, IL-1Ra), stimulators of fibroblast proliferation and matrix synthesis (IL-1β, TGF-β1), and markers of keratinocyte proliferation (keratins 5 and 6) and differentiation (small proline-rich proteins 2E and 1B). Moreover, this study is one of the first to demonstrate that kinetic gene expression profiling of whole organs can be correlated with morphological alterations in tissue, providing insight into the fundamental pathways that are responsible for disease initiation and progression. Data from recent reports and the current investigation support the hypothesis that, after allogeneic HSCT, IFN-γ is produced in the spleen and possibly other secondary lymphoid organs and functions in an endocrine manner to up-regulate proinflammatory gene expression in GVHD target organs.[31,32] Furthermore, as transplantation of IFN-$\gamma^{-/-}$ BM does not prevent recipient GVHD,[91,92] it appears that host-derived IFN-γ synthesized in the secondary lymphoid organs is sufficient to trigger target organ GVHD after allogeneic HSCT.

Acknowledgments

We thank Pete Ceuppens, David de Graaf, Jennifer L. Dube, Philip Jarvis, Julia Kozlovsky, Scott Wilkins, Lihua Yu, and Qi Zhang, all at AstraZeneca R&D Boston, for their contributions.

References

1. Ferrara JL, Deeg HJ: Graft-versus-host disease. N Engl J Med 1991, 324:667–674
2. Korngold B, Sprent J: Lethal graft-versus-host disease after bone marrow transplantation across minor histocompatibility barriers in mice. Prevention by removing mature T cells from marrow. J Exp Med 1978, 148:1687–1698
3. Ferrara J, Guillen FJ, Sleckman B, Burakoff SJ, Murphy GF: Cutaneous acute graft-versus-host disease to minor histocompatibility antigens in a murine model: histologic analysis and correlation to clinical disease. J Invest Dermatol 1986, 86:371–375
4. Cooke KR, Kobzik L, Martin TR, Brewer J, Delmonte Jr J, Crawford JM, Ferrara JL: An experimental model of idiopathic pneumonia syndrome after bone marrow transplantation: I. The roles of minor H antigens and endotoxin. Blood 1996, 88:3230–3239
5. Chudin E, Walker R, Kosaka A, Wu SX, Rabert D, Chang TK, Kreder DE: Assessment of the relationship between signal intensities and transcript concentration for Affymetrix GeneChip arrays. Genome Biol 2002, 3:RESEARCH0005
6. Murphy GF, Whitaker D, Sprent J, Korngold R: Characterization of target injury of murine acute graft-versus-host disease directed to multiple minor histocompatibility antigens elicited by either CD4+ or CD8+ effector cells. Am J Pathol 1991, 138:983–990
7. Gurish MF, Austen KF: The diverse roles of mast cells. J Exp Med 2001, 194:F1–F5
8. Denizot F, Brunet JF, Roustan P, Harper K, Suzan M, Luciani MF, Mattei MG, Golstein P: Novel structures CTLA-2 alpha and CTLA-2 beta expressed in mouse activated T cells and mast cells and homologous to cysteine proteinase proregions. Eur J Immunol 1989, 19:631–635
9. Holness CL, da Silva RP, Fawcett J, Gordon S, Simmons DL: Macrosialin, a mouse macrophage-restricted glycoprotein, is a member of the lamp/lgp family. J Biol Chem 1993, 268:9661–9666
10. Nagasawa R, Gross J, Kanagawa O, Townsend K, Lanier LL, Chiller J, Allison JP: Identification of a novel T cell surface disulfide-bonded dimer distinct from the alpha/beta antigen receptor. J Immunol 1987, 138:815–824
11. Yokoyama WM, Seaman WE: The Ly-49 and NKR-P1 gene families encoding lectin-like receptors on natural killer cells: the NK gene complex. Annu Rev Immunol 1993, 11:613–635
12. Freeman GJ, Gray GS, Gimmi CD, Lombard DB, Zhou LJ, White M, Fingeroth JD, Gribben JG, Nadler LM: Structure, expression, and T cell costimulatory activity of the murine homologue of the human B lymphocyte activation antigen B7. J Exp Med 1991, 174:625–631
13. Gilliam AC, Murphy GF: Cellular pathology of cutaneous graft-versus-host disease. Graft-Versus-Host Disease, Ed 2, Revised and Expanded. Edited by JLM DH Ferrara, SJ Burakoff. New York, Marcel Dekker, Inc., 1997, pp 291–314
14. Gilliam AC, Whitaker-Menezes D, Korngold R, Murphy GF: Apoptosis is the predominant form of epithelial target cell injury in acute experimental graft-versus-host disease. J Invest Dermatol 1996, 107:377–383
15. Graubert TA, Russell JH, Ley TJ: The role of granzyme B in murine models of acute graft-versus-host disease and graft rejection. Blood 1996, 87:1232–1237
16. Mebius RE: Organogenesis of lymphoid tissues. Nat Rev Immunol 2003, 3:292–303
17. Creagh EM, Conroy H, Martin SJ: Caspase-activation pathways in apoptosis and immunity. Immunol Rev 2003, 193:10–21
18. Lippens S, VandenBroecke C, Van Damme E, Tschachler E, Vandenabeele P, Declercq W: Caspase-14 is expressed in the epidermis, the choroid plexus, the retinal pigment epithelium and thymic Hassall's bodies. Cell Death Differ 2003, 10:257–259

19. Opferman JT, Korsmeyer SJ: Apoptosis in the development and maintenance of the immune system. Nat Immunol 2003, 4:410–415
20. Ong ST, Hackbarth ML, Degenstein LC, Baunoch DA, Anastasi J, McKeithan TW: Lymphadenopathy, splenomegaly, and altered immunoglobulin production in BCL3 transgenic mice. Oncogene 1998, 16:2333–2343
21. Cory S, Adams JM: The Bcl2 family: regulators of the cellular life-or-death switch. Nat Rev Cancer 2002, 2:647–656
22. Boehm U, Klamp T, Groot M, Howard JC: Cellular responses to interferon-gamma. Annu Rev Immunol 1997, 15:749–795
23. Boehm U, Guethlein L, Klamp T, Ozbek K, Schaub A, Futterer A, Pfeffer K, Howard JC: Two families of GTPases dominate the complex cellular response to IFN-gamma. J Immunol 1998, 161:6715–6723
24. Chu PG, Weiss LM: Keratin expression in human tissues and neoplasms. Histopathology 2002, 40:403–439
25. Mazzalupo S, Wong P, Martin P, Coulombe PA: Role for keratins 6 and 17 during wound closure in embryonic mouse skin. Dev Dyn 2003, 226:356–365
26. Steinert PM, Kartasova T, Marekov LN: Biochemical evidence that small proline-rich proteins and trichohyalin function in epithelia by modulation of the biomechanical properties of their cornified cell envelopes. J Biol Chem 1998, 273:11758–11769
27. Dinarello CA: Interleukin-1, interleukin-1 receptors and interleukin-1 receptor antagonist. Int Rev Immunol 1998, 16:457–499
28. Attisano L, Wrana JL: Signal transduction by the TGF-beta superfamily. Science 2002, 296:1646–1647
29. Diefenbach A, Jamieson AM, Liu SD, Shastri N, Raulet DH: Ligands for the murine NKG2D receptor: expression by tumor cells and activation of NK cells and macrophages. Nat Immunol 2000, 1:119–126
30. Mitsui G, Mitsui K, Hirano T, Ohara O, Kato M, Niwano Y: Kinetic profiles of sequential gene expressions for chemokines in mice with contact hypersensitivity. Immunol Lett 2003, 86:191–197
31. Ichiba T, Teshima T, Kuick R, Misek DE, Liu C, Takada Y, Maeda Y, Reddy P, Williams DL, Hanash SM, Ferrara JL: Early changes in gene expression profiles of hepatic GVHD uncovered by oligonucleotide microarrays. Blood 2003, 102:763–771
32. Baker KS, Allen RD, Roths JB, Sidman CL: Kinetic and organ-specific patterns of cytokine expression in acute graft-versus-host disease. Bone Marrow Transplant 1995, 15:595–603
33. Hill GR, Cooke KR, Teshima T, Crawford JM, Keith Jr JC, Brinson YS, Bungard D, Ferrara JL: Interleukin-11 promotes T cell polarization and prevents acute graft-versus-host disease after allogeneic bone marrow transplantation. J Clin Invest 1998, 102:115–123
34. Sykes M, Szot GL, Nguyen PL, Pearson DA: Interleukin-12 inhibits murine graft-versus-host disease. Blood 1995, 86:2429–2438
35. Hu HZ, Li GL, Lim YK, Chan SH, Yap EH: Kinetics of interferon-gamma secretion and its regulatory factors in the early phase of acute graft-versus-host disease. Immunology 1999, 98:379–385
36. Zhang Y, McCormick LL, Desai SR, Wu C, Gilliam AC: Murine sclerodermatous graft-versus-host disease, a model for human scleroderma: cutaneous cytokines, chemokines, and immune cell activation. J Immunol 2002, 168:3088–3098
37. New JY, Li B, Koh WP, Ng HK, Tan SY, Yap EH, Chan SH, Hu HZ: T cell infiltration and chemokine expression: relevance to the disease localization in murine graft-versus-host disease. Bone Marrow Transplant 2002, 29:979–986
38. Murphy GF, Sueki H, Teuscher C, Whitaker D, Korngold R: Role of mast cells in early epithelial target cell injury in experimental acute graft-versus-host disease. J Invest Dermatol 1994, 102:451–461
39. Christofidou-Solomidou M, Murphy GF, Albelda SM: Induction of E-selectin-dependent leukocyte recruitment by mast cell degranulation in human skin grafts transplanted on SCID mice. Am J Pathol 1996, 148:177–188
40. Klein LM, Lavker RM, Matis WL, Murphy GF: Degranulation of human mast cells induces an endothelial antigen central to leukocyte adhesion. Proc Natl Acad Sci USA 1989, 86:8972–8976
41. Walsh LJ, Trinchieri G, Waldorf HA, Whitaker D, Murphy GF: Human dermal mast cells contain and release tumor necrosis factor alpha, which induces endothelial leukocyte adhesion molecule 1. Proc Natl Acad Sci USA 1991, 88:4220–4224
42. Whitaker-Menezes D, Schechter NM, Murphy GF: Serine proteinases are regionally segregated within mast cell granules. Lab Invest 1995, 72:34–41
43. Kaminer MS, Lavker RM, Walsh LJ, Whitaker D, Zweiman B, Murphy GF: Extracellular localization of human connective tissue mast cell granule contents. J Invest Dermatol 1991, 96:857–863
44. Proudfoot AE: Chemokine receptors: multifaceted therapeutic targets. Nat Rev Immunol 2002, 2:106–115
45. Rossi D, Zlotnik A: The biology of chemokines and their receptors. Annu Rev Immunol 2000, 18:217–242
46. Loetscher P, Uguccioni M, Bordoli L, Baggiolini M, Moser B, Chizzolini C, Dayer JM: CCR5 is characteristic of Th1 lymphocytes. Nature 1998, 391:344–345
47. Koga S, Auerbach MB, Engeman TM, Novick AC, Toma H, Fairchild RL: T cell infiltration into class II MHC-disparate allografts and acute rejection is dependent on the IFN-gamma-induced chemokine Mig. J Immunol 1999, 163:4878–4885
48. Ryckman C, Vandal K, Rouleau P, Talbot M, Tessier PA: Proinflammatory activities of S100: proteins S100A8, S100A9, and S100A8/A9 induce neutrophil chemotaxis and adhesion. J Immunol 2003, 170: 3233–3242
49. Pratt JR, Basheer SA, Sacks SH: Local synthesis of complement component C3 regulates acute renal transplant rejection. Nat Med 2002, 8:582–587
50. Larson RS, Springer TA: Structure and function of leukocyte integrins. Immunol Rev 1990, 114:181–217
51. Wagner N, Lohler J, Kunkel EJ, Ley K, Leung E, Krissansen G, Rajewsky K, Muller W: Critical role for beta7 integrins in formation of the gut-associated lymphoid tissue. Nature 1996, 382:366–370
52. Huleatt JW, Lefrancois L: Antigen-driven induction of CD11c on intestinal intraepithelial lymphocytes and CD8+ T cells in vivo. J Immunol 1995, 154:5684–5693
53. Yang J, Galipeau J, Kozak CA, Furie BC, Furie B: Mouse P-selectin glycoprotein ligand-1: molecular cloning, chromosomal localization, and expression of a functional P-selectin receptor. Blood 1996, 87: 4176–4186
54. Borges E, Tietz W, Steegmaier M, Moll T, Hallmann R, Hamann A, Vestweber D: P-selectin glycoprotein ligand-1 (PSGL-1) on T helper 1 but not on T helper 2 cells binds to P-selectin and supports migration into inflamed skin. J Exp Med 1997, 185:573–578
55. Tovar V, de la Fuente MA, Pizcueta P, Bosch J, Engel P: Gene structure of the mouse leukocyte cell surface molecule Ly9. Immunogenetics 2000, 51:788–793
56. Sandrin MS, Gumley TP, Henning MM, Vaughan HA, Gonez LJ, Trapani JA, McKenzie IF: Isolation and characterization of cDNA clones for mouse Ly-9. J Immunol 1992, 149:1636–1641
57. Araki T, Zimonjic DB, Popescu NC, Milbrandt J: Mechanism of homophilic binding mediated by ninjurin, a novel widely expressed adhesion molecule. J Biol Chem 1997, 272:21373–21380
58. Moon AR, Oh GT, Kim JW, Choi YJ, Choe IS: Genomic DNA sequence and transcription factor binding sites of mouse ninjurin. DNA Seq 2001, 12:385–395
59. Springer TA: Traffic signals for lymphocyte recirculation and leukocyte emigration: the multistep paradigm. Cell 1994, 76:301–314
60. Springer TA: Adhesion receptors of the immune system. Nature 1990, 346:425–434
61. Ebnet K, Kaldjian EP, Anderson AO, Shaw S: Orchestrated information transfer underlying leukocyte endothelial interactions. Annu Rev Immunol 1996, 14:155–177
62. Bierer BE, Peterson A, Barbosa J, Seed B, Burakoff SJ: Expression of the T-cell surface molecule CD2 and an epitope-loss CD2 mutant to define the role of lymphocyte function-associated antigen 3 (LFA-3) in T-cell activation. Proc Natl Acad Sci USA 1988, 85:1194–1198
63. Gollob JA, Li J, Kawasaki H, Daley JF, Groves C, Reinherz EL, Ritz J: Molecular interaction between CD58 and CD2 counter-receptors mediates the ability of monocytes to augment T cell activation by IL-12. J Immunol 1996, 157:1886–1893
64. Chen CZ, Li M, de Graaf D, Monti S, Gottgens B, Sanchez MJ, Lander ES, Golub TR, Green AR, Lodish HF: Identification of endoglin as a functional marker that defines long-term repopulating hematopoietic stem cells. Proc Natl Acad Sci USA 2002, 99:15468–15473
65. Jonker L, Arthur HM: Endoglin expression in early development is associated with vasculogenesis and angiogenesis. Mech Dev 2002, 110:193–196
66. Schlegel PG, Vaysburd M, Chen Y, Butcher EC, Chao NJ: Inhibition of T cell costimulation by VCAM-1 prevents murine graft-versus-host disease across minor histocompatibility barriers. J Immunol 1995, 155:3856–3865

67. Li B, New JY, Yap EH, Lu J, Chan SH, Hu H: Blocking L-selectin and alpha4-integrin changes donor cell homing pattern and ameliorates murine acute graft versus host disease. Eur J Immunol 2001, 31:617–624
68. Kim JC, Whitaker-Menezes D, Deguchi M, Adair BS, Korngold R, Murphy GF: Novel expression of vascular cell adhesion molecule-1 (CD106) by squamous epithelium in experimental acute graft-versus-host disease. Am J Pathol 2002, 161:763–770
69. Norton J, Sloane JP: ICAM-1 expression on epidermal keratinocytes in cutaneous graft-versus-host disease. Transplantation 1991, 51: 1203–1206
70. Howell CD, Li J, Chen W: Role of intercellular adhesion molecule-1 and lymphocyte function-associated antigen-1 during nonsuppurative destructive cholangitis in a mouse graft-versus-host disease model. Hepatology 1999, 29:766–776
71. Masui T, Wakefield LM, Lechner JF, LaVeck MA, Sporn MB, Harris CC: Type beta transforming growth factor is the primary differentiation-inducing serum factor for normal human bronchial epithelial cells. Proc Natl Acad Sci USA 1986, 83:2438–2442
72. Wei L, Debets R, Hegmans JJ, Benner R, Prens EP: IL-1 beta and IFN-gamma induce the regenerative epidermal phenotype of psoriasis in the transwell skin organ culture system. IFN-gamma up-regulates the expression of keratin 17 and keratinocyte transglutaminase via endogenous IL-1 production. J Pathol 1999, 187:358–364
73. Lange A, Klimczak A, Karabon L, Suchnicki K: Cytokines, adhesion molecules (E-selectin and VCAM-1) and graft-versus-host disease. Arch Immunol Ther Exp (Warsz) 1995, 43:99–105
74. Davidson WF, Calkins C, Hugins A, Giese T, Holmes KL: Cytokine secretion by C3H-lpr and -gld T cells. Hypersecretion of IFN-gamma and tumor necrosis factor-alpha by stimulated CD4+ T cells. J Immunol 1991, 146:4138–4148
75. Gordon JR, Galli SJ: Promotion of mouse fibroblast collagen gene expression by mast cells stimulated via the Fc epsilon RI. Role for mast cell-derived transforming growth factor beta and tumor necrosis factor alpha. J Exp Med 1994, 180:2027–2037
76. Kendall JC, Li XH, Galli SJ, Gordon JR: Promotion of mouse fibroblast proliferation by IgE-dependent activation of mouse mast cells: role for mast cell tumor necrosis factor-alpha and transforming growth factor-beta 1. J Allergy Clin Immunol 1997, 99:113–123
77. Vesey DA, Cheung C, Cuttle L, Endre Z, Gobe G, Johnson DW: Interleukin-1beta stimulates human renal fibroblast proliferation and matrix protein production by means of a transforming growth factor-beta-dependent mechanism. J Lab Clin Med 2002, 140:342–350
78. Korngold R, Sprent J: Lethal GVHD across minor histocompatibility barriers: nature of the effector cells and role of the H-2 complex. Immunol Rev 1983, 71:5–29
79. Guillen FJ, Ferrara J, Hancock WW, Messadi D, Fonferko E, Burakoff SJ, Murphy GF: Acute cutaneous graft-versus-host disease to minor histocompatibility antigens in a murine model. Evidence that large granular lymphocytes are effector cells in the immune response. Lab Invest 1986, 55:35–42
80. Cerwenka A, Bakker AB, McClanahan T, Wagner J, Wu J, Phillips JH, Lanier LL: Retinoic acid early inducible genes define a ligand family for the activating NKG2D receptor in mice. Immunity 2000, 12:721–727
81. Cerwenka A, O'Callaghan CA, Hamerman JA, Yadav R, Ajayi W, Roopenian DC, Joyce S, Lanier LL: Cutting edge: the minor histocompatibility antigen H60 peptide interacts with both H-2Kb and NKG2D. J Immunol 2002, 168:3131–3134
82. Ferrara JL, Guillen FJ, van Dijken PJ, Marion A, Murphy GF, Burakoff SJ: Evidence that large granular lymphocytes of donor origin mediate acute graft-versus-host disease. Transplantation 1989, 47:50–54
83. van den Brink MR, Moore E, Horndasch KJ, Crawford JM, Hoffman J, Murphy GF, Burakoff SJ: Fas-deficient lpr mice are more susceptible to graft-versus-host disease. J Immunol 2000, 164:469–480
84. Larson MA, Wei SH, Weber A, Weber AT, McDonald TL: Induction of human mammary-associated serum amyloid A3 expression by prolactin or lipopolysaccharide. Biochem Biophys Res Commun 2003, 301:1030–1037
85. Huang JH, Liao WS: Synergistic induction of mouse serum amyloid A3 promoter by the inflammatory mediators IL-1 and IL-6. J Interferon Cytokine Res 1999, 19:1403–1411
86. Su SB, Gong W, Gao JL, Shen W, Murphy PM, Oppenheim JJ, Wang JM: A seven-transmembrane, G protein-coupled receptor, FPRL1, mediates the chemotactic activity of serum amyloid A for human phagocytic cells. J Exp Med 1999, 189:395–402
87. Sodin-Semrl S, Taddeo B, Tseng D, Varga J, Fiore S: Lipoxin A4 inhibits IL-1 beta-induced IL-6, IL-8, and matrix metalloproteinase-3 production in human synovial fibroblasts and enhances synthesis of tissue inhibitors of metalloproteinases. J Immunol 2000, 164:2660–2666
88. Aliberti J, Serhan C, Sher A: Parasite-induced lipoxin A4 is an endogenous regulator of IL-12 production and immunopathology in Toxoplasma gondii infection. J Exp Med 2002, 196:1253–1262
89. Gewirtz AT, Collier-Hyams LS, Young AN, Kucharzik T, Guilford WJ, Parkinson JF, Williams IR, Neish AS, Madara JL: Lipoxin a4 analogs attenuate induction of intestinal epithelial proinflammatory gene expression and reduce the severity of dextran sodium sulfate-induced colitis. J Immunol 2002, 168:5260–5267
90. Jozsef L, Zouki C, Petasis NA, Serhan CN, Filep JG: Lipoxin A4 and aspirin-triggered 15-epi-lipoxin A4 inhibit peroxynitrite formation, NF-kappa B and AP-1 activation, and IL-8 gene expression in human leukocytes. Proc Natl Acad Sci USA 2002, 99:13266–13271
91. Ellison CA, Fischer JM, HayGlass KT, Gartner JG: Murine graft-versus-host disease in an F1-hybrid model using IFN-gamma gene knockout donors. Immunol 1998, 161:631–640
92. Murphy WJ, Welniak LA, Taub DD, Wiltrout RH, Taylor PA, Vallera DA, Kopf M, Young H, Longo DL, Blazar BR: Differential effects of the absence of interferon-gamma and IL-4 in acute graft-versus-host disease after allogeneic bone marrow transplantation in mice. J Clin Invest 1998, 102:1742–1748